

Chaos-induced intrinsic localized modes in coupled microcantilever arrays

Qingfei Chen,^{1,a)} Liang Huang,¹ and Ying-Cheng Lai^{1,2}

¹Department of Electrical Engineering, Arizona State University, Tempe, Arizona 85287, USA

²Department of Physics and Astronomy, Arizona State University, Tempe, Arizona 85287, USA

(Received 13 February 2008; accepted 26 May 2008; published online 18 June 2008)

We find that intrinsic localized modes (ILMs) in microelectromechanical cantilever arrays can be induced by the spatiotemporal chaos dynamics. For typical settings, spatiotemporal chaos is ubiquitous and can act as a natural platform for ILMs to arise. Our study suggests an experimental approach to preventing ILMs, i.e., to choose the modulation frequency so as to place the system in a regime where there is a low energy stable state. © 2008 American Institute of Physics. [DOI: 10.1063/1.2946494]

The energy output of a microelectromechanical (MEM) and nanoelectromechanical (NEM) system can be significantly enhanced by a coupled array structure, providing a viable solution to the critical problem of achieving high energy output in micro- and nanosize devices. The collective behavior of coupled MEMS (NEMS) arrays can also efficiently enhance the performance of resonator-based devices, such as rf filters,¹ mass sensors,² magnetometers,³ etc.

The occurrence of energy localization in MEM arrays has been discovered recently.⁴ Such localized energy excitations, called *intrinsic localized modes* (ILMs), also known as “discrete breathers” or “lattice solitons,” can occur in a defect-free mechanically coupled microcantilever arrays, extending over only a few sites. The advances in silicon and optical visualization technologies render feasible detailed experimental studies of ILMs in MEM systems, making them a paradigm for investigating the fundamentals of this interesting nonlinear phenomenon. In device applications, ILMs may be undesirable. In particular, since ILM features delta functionlike shape in space, it can induce large spatial heterogeneity and therefore can cause damage and fatigue to the device. An interesting question is that under what conditions can ILMs occur in MEM (NEM) arrays? A related issue concerns experimental strategies to eliminate ILMs. For instance, suppose the device modulation frequency is a control experimental parameter that can be adjusted conveniently in experiment. In what regime should the frequency be so that ILMs do not occur? In previous studies,⁴⁻⁶ it was thought that ILMs are triggered by temporal noise and frequency modulation. However, we find that, besides of noise, ILMs can also be excited from inherent spatiotemporal chaotic motion in MEM arrays. Our study suggests an effective approach to avoid ILMs by properly tuning the driven frequency to a “safe” low energy state regime.

The geometry of the coupled cantilevers employed in the experimental study⁴ is shown in Fig. 1 where two cantilevers of alternating length are coupled by an overhang. The MEM arrays are fabricated by low-stress silicon nitride and is driven by a piezoelectric transducer. The material properties of the experimental device are^{5,8} $L_1=50\ \mu\text{m}$, $L_2=55\ \mu\text{m}$, $W_1=W_2=15\ \mu\text{m}$, $T=0.3\ \mu\text{m}$, $H=23\ \mu\text{m}$, and $P=40\ \mu\text{m}$. The density and Young’s modulus of the material are $\rho=2300\ \text{kg/m}^3$ and $E=110\ \text{GPa}$, respectively.

The dynamics of a MEM cantilever beam is, in general, described by a sophisticated nonlinear partial differential equation⁷ that involves complicated mechanical and electrical interactions between the beam and its surroundings. For a single cantilever beam, the continuum equation of motion under driving force is⁵ $\rho A(\partial^2 u/\partial t^2) + EI(\partial^4 u/\partial s^4) + EI(\partial/\partial s) \times [\partial u/\partial s \partial/\partial s(\partial u/\partial s \partial^2 u/\partial s^2)] = \rho A \alpha \cos \Omega t$, where $A=WT$ is the cross-sectional area of the beam and $I=(WT^3)/12$ is the moment of inertia. The displacement variable $u(s,t)$ can be expanded on a set of orthonormal shape functions, $\phi_n(s)$ of frequency ω_n : $u(s,t) = \sum_n \phi_n(s) \chi_n(t)$, where $\chi_n(t)$ is the beam tip’s displacement. The shape functions satisfy the boundary conditions $\phi_n(0)=0$ and $\phi_n(L)=1$. Substituting this expansion into the continuum beam equation and keeping only the lowest frequency mode, one obtains an ordinary differential equation: $m d^2/dt^2 x(t) + k_2 x(t) + k_4 x(t)^3 = m \alpha \cos \Omega t$, where $x(t)$ is the displacement of the beam’s tip, $k_2=(12.36EI)/L^3$ is the harmonic spring constant, and $k_4=(24.79EI)/L^5$ is the quadratic spring constant. For coupled microcantilever arrays, the dynamical equation is more complicated. The cantilevers are affected by damping environment and they interact with each other by coupling force. The system equation of motion can be described by $m_i \ddot{x}_i + b_i \dot{x}_i + k_{2i} x_i + k_{4i} x_i^3 + k_l(2x_i - x_{i+1} - x_{i-1}) = m_i \alpha \cos(2\pi f t)$, where x_i ($i=1, \dots, N$) is the displacement of the end point of the i th cantilever beam of effective mass m_i , b_i is the damping coefficient, k_{2i} and k_{4i} are the on-site harmonic and quadratic spring constants of the i th beam, respectively, and k_l is the harmonic coupling spring constant determined by the structure of coupling overhangs. Each beam is subject to a common sinusoidal driving characterized by acceleration α and modulation frequency f . In our numerical experiments, there are $N=256$ beams of alternating length. While the parameters of the dynamical

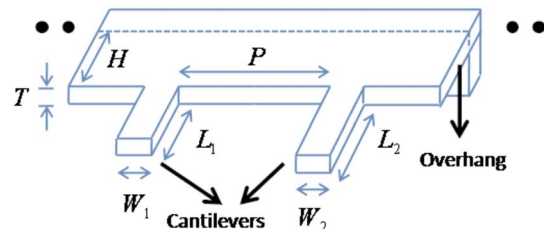


FIG. 1. (Color online) Schematic diagram of the coupling MEM cantilevers. $L_1, L_2, W_1, W_2, T, P,$ and H denote the beams’ lengths, widths, thicknesses, the length of pitch, and the length of overhang, respectively.

^{a)}Electronic mail: chenqingfei_03@hotmail.com.

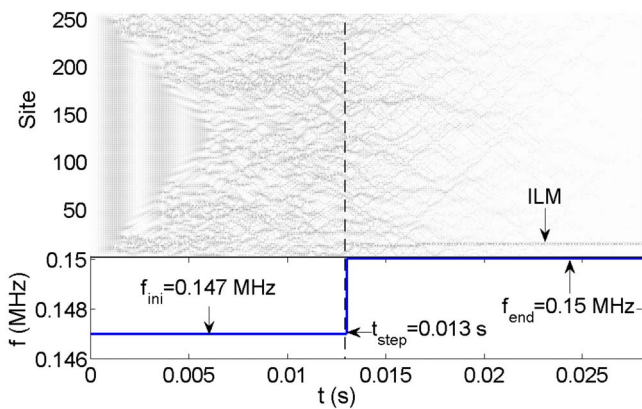


FIG. 2. (Color online) For $k_f=0.0241$ N/m and $\alpha=1.56 \times 10^4$ m/s², spatiotemporal chaos in a microcantilever array of $N=256$ beams. The driving frequency is increased abruptly from 1.47×10^5 Hz to 1.50×10^5 Hz at $t_{\text{step}}=0.013$ s.

equation for the beams can be obtained by theoretical considerations, for real device the nonideal operation environment and fabrication errors will affect the values of parameters so corrections are needed for accurate numerical simulation. For example, in Ref. 4, an estimation technique is used by fitting the results from the dynamical equations such as the dispersion curve, shift of the upper branch of frequency, the decay rate, etc., to their experimental counterparts. A set of parameters estimated by this technique is as follows:⁴ $(m_i, b_i, k_{2i}, k_{4i}) = (5.46 \times 10^{-13}$ kg, 6.24×10^{-11} kg/s, 0.303 N/m, 5×10^8 N/m³) for odd i , the long beams, $(m_i, b_i, k_{2i}, k_{4i}) = (4.96 \times 10^{-13}$ kg, 5.67×10^{-11} kg/s, 0.353 N/m, 5×10^8 N/m³) for even i , the short beams, and $k_f=0.0241$ N/m. These parameters are used in our study.

In previous works on microcantilever array with alternating beam length,^{4,6,8} it has been argued that in order for ILMs to occur (1) the initial state of the microcantilever array should be random to allow for spatial heterogeneity, and (2) when the heterogeneity of initial state (or temporal noise) is small, the frequency of the external driving should be increased with time (frequency chirping) to amplify the small heterogeneity. Our studies reveal, however, that both conditions can be relaxed. In particular, the degree of heterogeneity in the initial-condition distribution can be made arbitrarily small. For instance, we can actually use zero initial conditions for all beams. The phenomenon is that *spatiotemporal chaos* can occur typically in the parameter regime of low driving frequency due to the uneven distribution of the beam length, which can serve as the source of spatial heterogeneity for beam dynamics. Because of chaos, the required frequency chirping scheme can be replaced by frequency switching. Qualitatively, this can be seen by noting that chaos contains an infinite number of possibilities for dynamical state. Once the system is in a chaotic regime, a change in the driving frequency can “fix” the system in one of the ILM states. Depending on the amount of frequency change, different ILMs can occur physically.

Figure 2 presents a space-time plot of the amplitudes of oscillating beams in the same system that has been used in previous experimental and numerical studies.⁴ The initial displacements and velocities are all set to be zero. Figure 2 reveals a highly irregular behavior before $t_{\text{step}}=0.013$ s, both in space and in time, which is a characteristic of spatiotem-

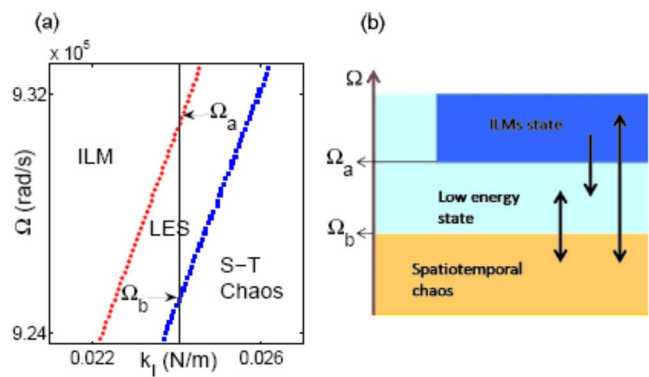


FIG. 3. (Color online) (a) For a microcantilever array of $N=256$ beams, in a two-dimensional, experimentally accessible parameter region, boundaries between various asymptotic states including spatiotemporal chaos and various ILMs. (b) A schematic illustration of allowed and forbidden transitions between various states in a MEM oscillator array by frequency control.

poral chaos. Indeed, analysis of time series and spatial plots of dynamical variables point to chaos, which has been found to be independent of the number of beams in the system, insofar as it is more than a few. At t_{step} , the driving frequency is tuned up, generating an ILM at site 14. This result shows that with the heterogeneity brought upon by spatiotemporal chaos, ILMs can occur even in a noise-free system with uniform initial conditions.

To explain the mechanism for the generation of ILMs by chaos, we simplify the dynamic model by standard averaging method.⁹ Let $\Omega=2\pi f$, $x_i(t)=U_i(t)\cos(\Omega t)+V_i(t)\sin(\Omega t)$, and define $Q_i=\sqrt{m_i k_{2i}}/b_i$ as the quality factor, $\Omega_{0i}=\sqrt{k_{2i}/m_i}$ as the resonant frequency of beam i . The averaged functions of $U_i(t)$ and $V_i(t)$, denoted by $u_i(t)$ and $v_i(t)$, respectively, satisfy $du_i/dt=-1/2\Omega[(\Omega^2-\Omega_{0i}^2)v_i-\frac{3}{4}(k_{4i}/m_i)v_i(u_i^2+v_i^2)+(\Omega_{0i}/Q_i)\Omega u_i-k_f/m_i(2v_i-v_{i+1}-v_{i-1})]$, $dv_i/dt=1/2\Omega[(\Omega^2-\Omega_{0i}^2)u_i-\frac{3}{4}(k_{4i}/m_i)u_i(u_i^2+v_i^2)-(\Omega_{0i}/Q_i)\Omega v_i+\alpha-k_f/m_i(2u_i-u_{i+1}-u_{i-1})]$, $i=1, \dots, N$. In this model, the transition to ILM state from chaos can be understood. As the coupling parameter is increased from zero, two types of bifurcation can occur that cause a stable equilibrium to lose its stability: saddle-node and stability-transition bifurcations. A numerical bifurcation analysis indicates that the high-amplitude oscillation mode usually loses stability earlier than the low-amplitude mode as k_f is increased. Thus, for sufficiently large values of k_f when the low-amplitude oscillations lose their stabilities, there are no longer stable orbits in the system. In fact, all equilibrium points and periodic orbits are unstable, and a network of homoclinic and heteroclinic crossings arises, which generates horseshoe dynamics and henceforth chaos.⁹ Extensive computations reveal that when the system is in chaos, increasing the driving frequency will typically land the system in one of the ILMs. It is in this sense that we say chaos provides a natural platform for ILMs through frequency control.

To further explore the chaos route to ILMs, it is useful to focus on the two-dimensional parameter space (k_f, Ω) , which is experimentally accessible. To facilitate test of our predictions, we choose the ranges of the parameters as in typical experiments.^{4,5,8} Figure 3(a) shows, for a system of $N=256$ beams, boundaries between distinct asymptotic states including spatiotemporal chaos and various ILMs. In the figure, the region to the right of the “square” boundary is for spatiotemporal chaos, the region to the left denotes the “low energy

state” (LES) where the low energy oscillation mode is stable but the ILMs modes are unstable. ILMs can be expected in the region to the left of the “circle” boundary. Figure 3 indicates that, for example, LES and ILM states are both possible in the parameter region to the left of the circle boundary. For a given set of parameter values, distinct oscillation states have different basins of attraction in the phase space. Now imagine an experimental situation where k_f is fixed and the driving frequency is increased, as indicated by the vertical line in Fig. 3 where Ω_b and Ω_a are the intersections between the dashed line and the boundaries of LES and ILMs, respectively. For $\Omega < \Omega_b$, the system has no stable equilibrium and it exhibits spatiotemporal chaos. For $\Omega_a > \Omega > \Omega_b$, there is one stable equilibrium in the averaged system, corresponding to stable oscillations of low energy in the actual system. In this case, all initial conditions generate trajectories that approach this LES. For $\Omega > \Omega_a$, both LES and ILM states are possible. That is, depending on the choice of initial conditions, all beams in the system can oscillate with low amplitude or the system can exhibit at least one ILM in the space.

How do ILMs occur from spatiotemporal chaos? Figure 3(b) illustrates the mechanism: If the system state is in spatiotemporal chaos regime where $\Omega < \Omega_b$ and the frequency is increased to above Ω_a , ILMs can occur. Suppose now the frequency is reduced to some value in the region of $\Omega \in [\Omega_b, \Omega_a]$, the system will then be in a LES. Equivalently, we say there is a transition from an ILM state to a LES. A key point is that it is practically impossible to change the system back into the ILM state from the LES by increasing the frequency from some value in between Ω_b and Ω_a to some value above Ω_a . The reason is that, once the system settles down in a LES, the amount of spatial heterogeneity is not sufficient for ILMs to arise so that it will always be in the basin of LES, regardless of any frequency increase. In this sense, the transition from LES to ILM state is forbidden, which means that the LES regime is a *safe* frequency regime of ILMs. This line of reasoning suggests that in the absence of any random factors, *the only way to excite the system to an ILM state is through spatiotemporal chaos*. Thus, even for a noiseless system, spatiotemporal chaos provides a natural platform for exciting ILMs in microcantilever arrays. This analysis also suggests that one can always eliminate ILMs by tuning the frequency to LES regime and then restore the original frequency. That is, LES serves as a natural ILMs terminator in MEM (NEM) arrays. Computational results are shown in Fig. 4 to illustrate this mechanism. For comparison, we show in Fig. 4(a) an example where the final state of the system is a LES. In particular, the operation frequency is enhanced from f_{ini} to f_2 (which is in the LES regime) at time t_1 . The result shows that the motions of all beams decay to

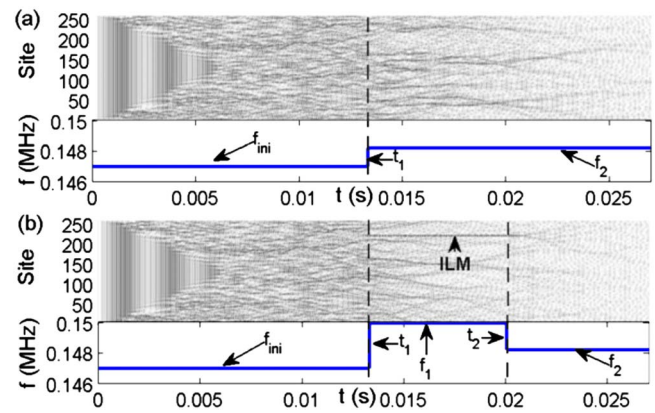


FIG. 4. (Color online) Spatiotemporal plots for $k_f=0.0241$ N/m and $\alpha=1.56 \times 10^4$ m/s². Two examples where (a) the system is driven to LES and (b) the system is first driven to ILM state and then to LES.

LES and no ILM occurs. Figure 4(b) shows a case where an ILM is first excited and locked at site 220 by changing the frequency from f_{ini} to f_1 in the ILM regime. After some amount of time, the frequency is tuned down to f_2 at time t_2 . The ILM then decays and the system exhibits a LES.

In conclusion, we find that spatiotemporal chaos occurs commonly in MEM arrays providing necessary space heterogeneity for exciting ILMs. Initial noise and special frequency modulation scheme are not required for exciting ILMs. To prevent ILMs, the driven frequency should be in the region, where LES is stable and our analysis yields specific parameter regime for eliminating ILMs, which are experimentally accessible.

This work was supported by AFOSR under Grant No. FA9550-06-1-0024.

¹M. U. Demirci, M. A. Abdelmoneum, and C. T.-C. Nguyen, Digest of Technical Papers, The 12th International Conference on Solid-State Sensors and Actuators (Transducers'03), Boston, MA, 8–12 June 2003 (unpublished), pp. 955–958.

²B. Ilic, H. G. Craighead, S. Krylov, W. Senarathne, C. Ober, and P. Neuzil, *J. Appl. Phys.* **95**, 3694 (2004); K. L. Ekcini, X. M. H. Huang, and M. L. Roukes, *Appl. Phys. Lett.* **84**, 4469 (2004).

³D. K. Wickenden, J. L. Champion, R. Osiander, R. B. Givens, J. L. Lamb, J. A. Miragliotta, D. A. Oursler, and T. J. Kistenmacher, *Acta Astronaut.* **52**, 421 (2003).

⁴M. Sato, B. E. Hubbard, A. J. Sievers, B. Ilic, D. A. Czaplewski, and H. G. Craighead, *Phys. Rev. Lett.* **90**, 044102 (2003).

⁵M. Sato, B. E. Hubbard, and A. J. Sievers, *Rev. Mod. Phys.* **78**, 137 (2006).

⁶P. Maniatis and S. Flach, *Europhys. Lett.* **74**, 452 (2006).

⁷M. Sato, B. E. Hubbard, L. Q. English, A. J. Sievers, B. Ilic, D. A. Czaplewski, and H. G. Craighead, *Chaos* **13**, 702 (2003).

⁸S. K. De and N. R. Aluru, *Phys. Rev. Lett.* **94**, 204101 (2005); *J. Microelectromech. Syst.* **15**, 355 (2006).

⁹J. Guckenheimer and P. Holmes, *Nonlinear Oscillations, Dynamical Systems, and Bifurcations of Vector Fields* (Springer, New York, 1990).